SUPPLEMENTARY DATA

1.0 Poly-L-Glutamic Acid – [5-^{3}H]-2′-Deoxycytidine (PG-[^{3}H]dCyd, *PG)

1.1 Development and optimization of conjugation method of [5-^{3}H]-2′-Deoxycytidine to the poly-L-glutamic acid (using non-radioactive 2′-Deoxycytidine as a model)

In the current study, the tritium (^{3}H) labelling of poly-L-glutamic acid (PG) was done via conjugating [5-^{3}H]-2′-Deoxycytidine to the poly-L-glutamic acid. To reduce the use of radioactive compound during the method development / optimization phase, the non-radioactive 2′-Deoxycytidine was chosen instead of the [5-^{3}H]-2′-Deoxycytidine.

The reaction to produce PG-dCyd conjugate was based on an earlier procedure described for the preparation of poly-L-glutamic acid – gemcitabine[1, 2] and *PG. Briefly, 10 mg PG (0.077 mmol), 0.05 mg deoxycytidine (dCyd, 0.2 μmol), 10 mg dicyclohexylcarbodiimide (DCC, 0.048 mmol) and 0.1 mg dimethylaminopyridine (DMAP) were added to 2 mL dry N,N-dimethylformamide (DMF) in a small dried reaction flask under dry nitrogen atmosphere and stirred. The product was then isolated and characterized by 1H and 13C nuclear magnetic resonance (NMR) spectroscopy. The purity of PG-dCyd and dCyd in PG-dCyd were determined using high performance liquid chromatography (HPLC) as described earlier for PG[1]. Briefly, the HPLC system consisted of a Waters 2690 solvent delivery module, a Waters 996 PDA (Waters Co., Milford, MA, USA), a Microsorb-MV 100-5 C18 RP-HPLC column (4.6 mm × 250 mm, 280 Å, 5 μm ODS coated silica gel particles, Varian Inc., Palo Alto, CA, USA) and a Waters millennium v3.02 workstation. The composition of the mobile phase to determine the content of dCyd in the synthesized PG-dCyd and purity of PG-dCyd was 0.02 M ammonium acetate (0.02 M AMN)/acetonitrile

(ACN) (1:1) with a flow rate of 0.5 mL/min. The sampling volume was 10 μL and the UV wavelength was set at 268 nm.

The results indicate the lyophilisation of the final dialysate yielded 8.1 mg of product as a white powder (yield = 81%). HPLC analysis using a mobile phase of 0.02 M AMN/ACN (1:1) showed no free dCyd or other UV light-absorbing contaminants present in the synthesized PG-dCyd conjugate. Under these HPLC conditions, the free dCyd was represented by a peak at the retention time of 4.22 min, while the bound dCyd in PG-dCyd was represented by a peak at 3.34 min (Figure 1). The content of bound dCyd in PG-dCyd estimated was 5 % w/w.

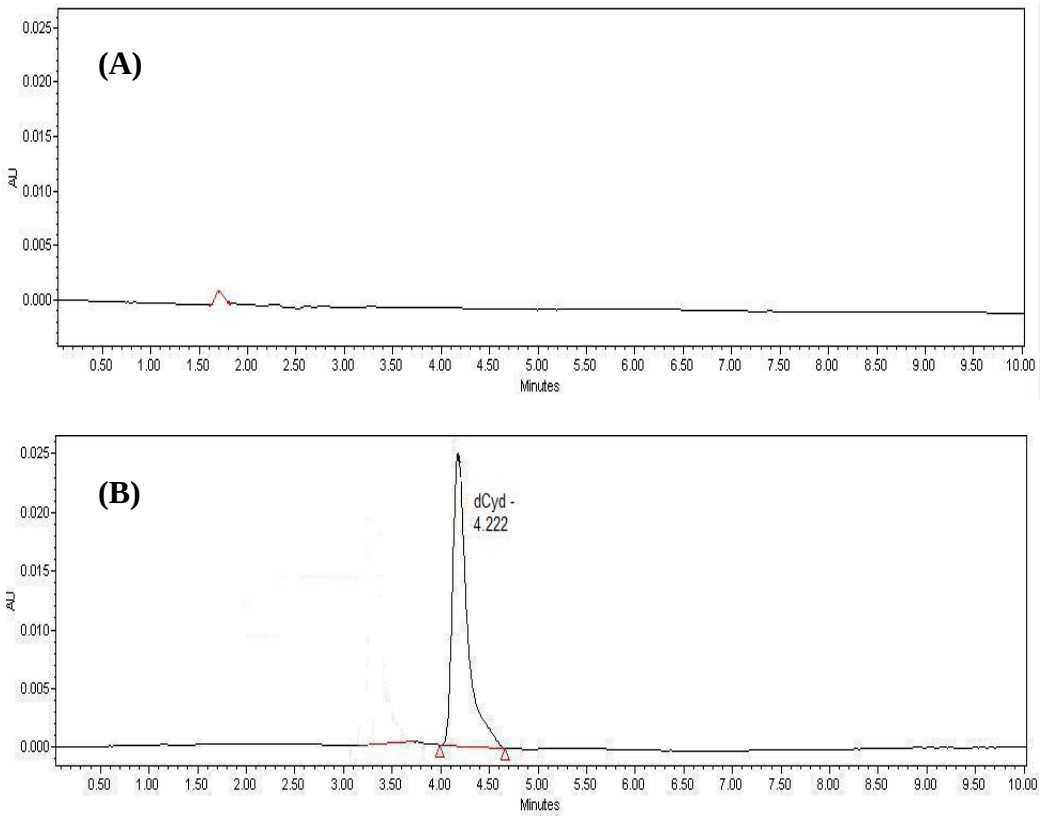

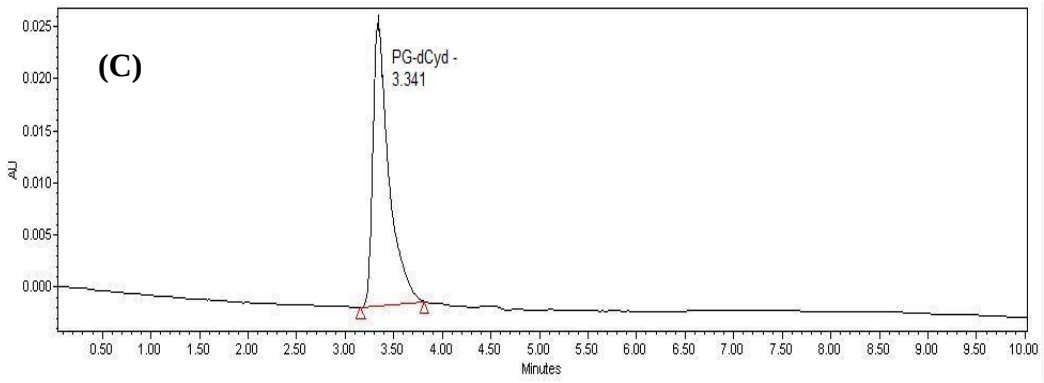

Figure 1 The HPLC chromatograms of (A) 1 mg/mL PG, (B) 0.05 mM dCyd, (C) 1 mg/mL PG-dCyd.

Abbreviation: HPLC, high performance liquid chromatography; PG, poly-L-glutamic acid sodium salt; dCyd, 2′-deoxycytidine; PG-dCyd, poly-L-glutamic acid – 2′-deoxycytidine

^{1}H and ^{13}C NMR analyses were performed on the PG-dCyd conjugate that was synthesized, as well as on dCyd and PG polymer in the proton form, to elucidate the molecular structure of PG-dCyd and to identify the side group that was involved in the conjugation reaction. The ^{1}H and ^{13}C chemical shifts of dCyd and PG NMR spectra were assigned and were consistent with previously published values[1, 2] (Figure 2). Thus, based on the successful conjugation of dCyd to PG, we prepared *PG for biodistribution studies in normal and streptozocin-induced diabetic rats.

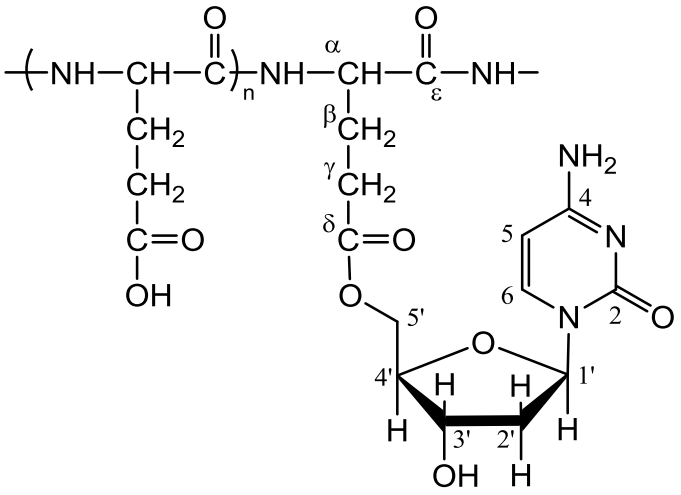

Figure 2 Poly-L-glutamic acid – deoxycytidine (PG-dCyd).

^{1}H NMR (D_2O) of deoxycytidine (dCyd), δ (ppm): 7.79 (d, 1H, H–6), 6.23 (t, 1H, H–1’), 6.00 (d, 1H, H–5), 4.40 (dt, 1H, H–3’), 4.02 (dt, 1H, H–4’), 3.80 (dd, 1H, H–5_a’), 3.72 (dd, 2H, H–5_b’), 2.39 (ddd, 1H,H–2_a’), 2.25 (dt, 1H, H–2_b’); ^{13}C NMR (D_2O), δ (ppm): 166.13 (C–2), 157.52 (C–4), 141.49(C–6), 96.20 (C–5), 86.62 (C–1’), 86.12(C–4’), 70.55 (C–3’), 61.28 (C–5’), 39.30 (C–2’).

^{1}H NMR (D_2O) of PG (proton form), δ (ppm): 4.25 (dd, 1H, H–α), 2.22 (m, 2H, H–γ), 1.98 (m, 1H, H–$\beta_{a,}$), 1.88 (m, 1H, H–$\beta_{b,}$);^{13}C NMR (D_2O), δ (ppm): 182.10 (C–δ), 174.15 (C–ε), 54.10 (C–α), 34.23 (C–γ), 28.67 (C–β).

^{1}H NMR (D_2O) of PG-dCyd, δ (ppm): 8.57 (br s, 1H, PG-NHCO), 7.80 (d, 1H, H–6), 6.24(t, 1H,H–1′), 6.02 (d, 1H, H–5), 4.41 (dt, 1H, H–3’), 4.28 (dd, 1H, H–α), 4.02 (dt, 1H, H–4’), 3.62 (dd, 1H, H–5_a′), 3.53 (dd, 1H, H–5_b′), 2.40 (ddd, 1H, H–2_a’), 2.24 (m, 3H, H–2_b’, H–γ), 2.00 (m, 1H, H–β_a), 1.89 (m, 1H, H–β_b); ^{13}C NMR (D_2O), δ (ppm): 182.14 (C–δ), 174.12 (C–ε), 166.69 (C–2), 158.11 (C–4), 142.15 (C–6), 96.85 (C–5), 87.22 (C–1’), 86.70 (C–4’), 71.16 (C–3’), 61.89 (C-5’), 54.06 (C–α), 39.84 (C–2’), 34.22 (C–γ), 28.68 (C–β).

The NMR spectra indicated that the conjugation of dCyd to PG occurred through the formation of an ester bond between the –OH at C-5' position of dCyd and the –COOH at C–δ position of PG. This was supported by the upfield shift of the H-5' dCyd peaks from 3.80 and 3.72 ppm in the ^{1}H NMR of dCyd spectrum to 3.62 and 3.53 ppm, respectively, in the PG-dCyd spectrum. This phenomenon is probably due to the anisotropy shielding effect of the neighbouring carbonyl group of the ester formed by the conjugation reaction.

1.2 Stability of PG-dCyd in Plasma

The plasma stability of *PG was determined using PG-dCyd as a model compound. PG-dCyd was incubated in fresh human plasma for up to 120 h at 37°C. EDTA anticoagulated whole blood was centrifuged at 1300 x *g*, at 4°C for 10 min to extract the human plasma. PG-dCyd (10 mg) was dissolved in 10 mL human plasma at pH 7.4 and incubated at 37°C for 5 days. Aliquots (500 μL) were sampled at various time points (0, 0.5, 1, 2, 4, 6, 8, 12, 24, 48, 72, 96 and 120 h) and subjected to an optimised, pre-validated filter-extraction protocol prior to high performance liquid chromatography (HPLC) analysis. The filtrates were then analysed using HPLC to estimate the release of dCyd from PG backbone over 120 h.

The plasma aliquots were then subjected to an optimised, prevalidated filter-extraction protocol prior to HPLC analysis. Briefly, 500 μL of PG-dCyd or dCyd-containing plasma aliquot was filtered using an Amicon Microcon centrifugal filter device (Millipore, Billerica, MA, USA, 10,000 molecular weight cut off point, centrifugal filtration at 14,000 x *g* for 1 h) to remove any macromolecules that might block the HPLC column, and any UV absorbing macromolecules that might interfere with the dCyd content determination. The filtrates were

then analysed using the HPLC described earlier,[1] except the mobile phase was 0.02 M AMN/ACN (9:1). The sampling volume was 10 μL and monitored at 268 nm.

The protocol for the centrifugal-filter extraction-HPLC assay for the analysis of plasma degradation of gemcitabine was validated using six replicates. The limit of quantification (LOQ) of dCyd in plasma was 0.01 mM. The calibration curve, between 0.01 and 1.00 mM dCyd, was constructed and its linearity determined (R^2 = 0.997). The intra-day and inter-day precision of the concentrations of dCyd at 0.10, 0.50 and 1.00 mM was < 15% RSD, whereas the recoveries of dCyd at the same concentrations were above 97%. The retention times for plasma, dCyd and dCyd degradation product were 4.74, 5.50 and 6.45 min, respectively (Figure 3).

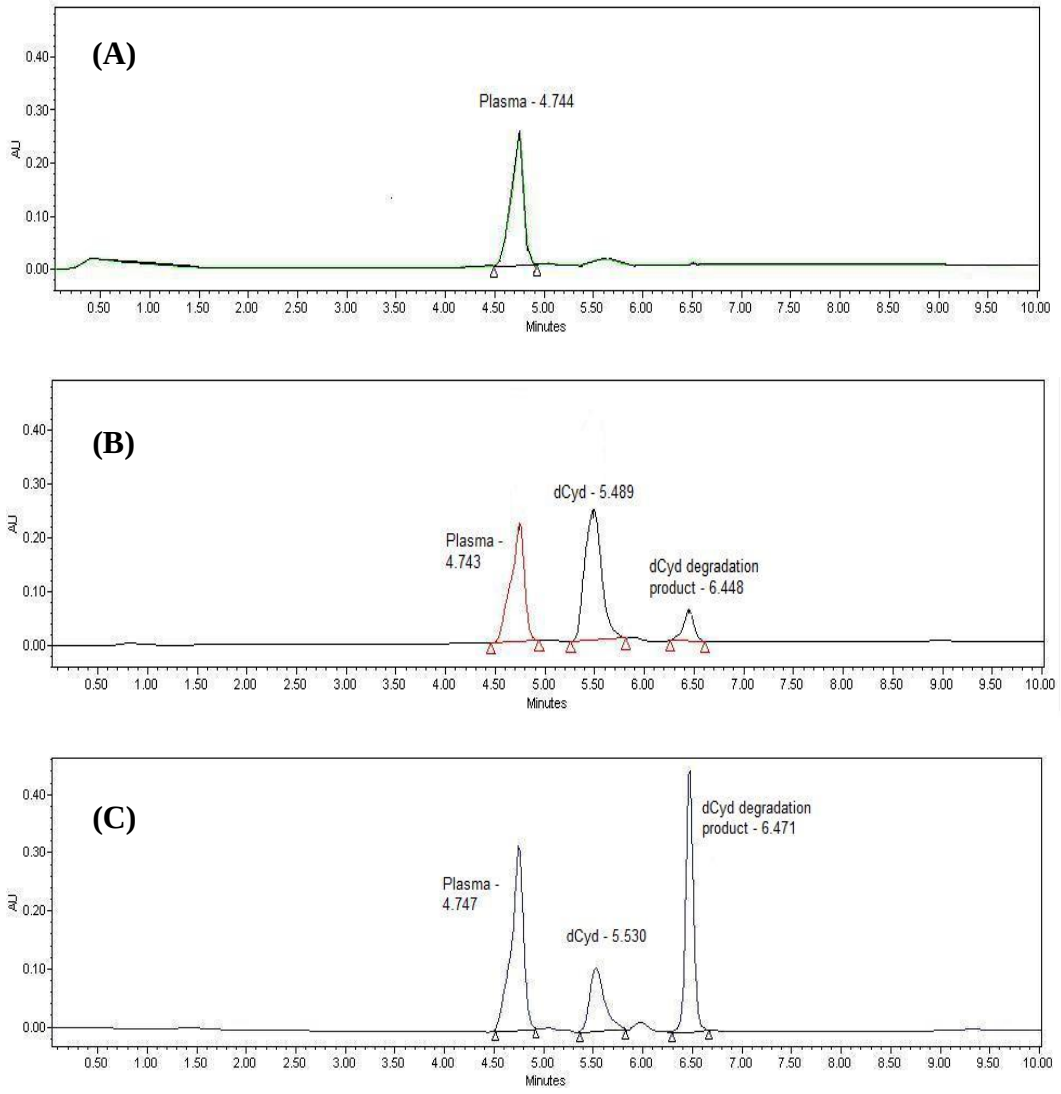

Figure 3 The HPLC chromatograms of (A) blank plasma sample, (B) plasma sample spiked with 0.2 mM dCyd, (C) plasma sample spiked with 0.2 mM dCyd and incubated at 37 °C for 24 h.

Abbreviation: HPLC, high performance liquid chromatography; dCyd, 2′-deoxycytidine

The results showed that the onset of dCyd release (1%) from PG-dCyd was at 24 h, followed by 10% release at 48 h and 30% release at 72 h (Figure 4). Maximum dCyd release (80%) was at 96 h. Prior to 24 h, no significant increase of dCyd was noted in plasma, indicating the stability of PG-dCyd in plasma at 37°C lasted for at least 24 h. Based on the results, the biodistribution monitoring of PG-[^{3}H]-dCyd was set to be performed for a period of up to 24 h (Figure 4).

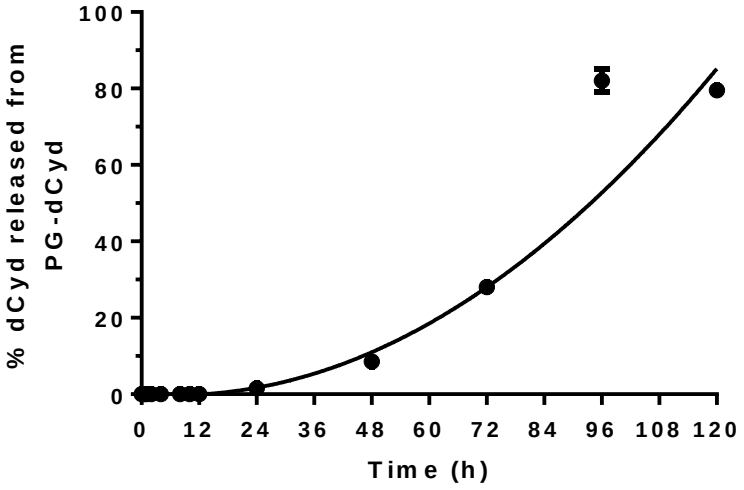

Figure 4 Time dependent release of dCyd from PG-dCyd in plasma at 37°C over a period of 120 h

Abbreviation: dCyd, 2′-deoxycytidine; PG-dCyd, poly-L-glutamic acid – 2′-deoxycytidine

2.0 Characterization of Poly-L-Glutamic Acid – 4-(2-Aminoethyl) Benzenesulfonyl Fluoride (PG-AEBSF)

The NADPH oxidase inhibitor, 4-(2-aminoethyl)benzenesulfonyl fluoride (AEBSF), was conjugated to poly-L-glutamic acid (PG)(method as described in main text). The yield of PG-AEBSF was calculated. The product was further characterized by ^{1}H and ^{13}C nuclear

magnetic resonance (NMR) spectroscopy. The purity of the PG-AEBSF and AEBSF content in PG-AEBSF was determined using a HPLC system consisting of an online degasser DGU-14A, an auto sampler SIL-20A HT, a gradient pump LC-10AD, a column oven CTO-10A, an UV detector SPD-10A, a fluorescence detector RF-10A XL and a communicator module CBM-20A (Shimadzu Corporation, Kyoto, Japan). The column was Microsorb-MV 100-5 C18 (4.6 mm x 250 mm, 280Å, 5 mm ODS coated silica gel particles, Varian Inc., Palo Alto, CA, USA). A mobile phase of acetonitrile and 0.1% trifluoroacetic acid (40:60) at a flow rate of 1 mL/min was used for the HPLC analysis. The sample volume was 10 μL and monitored at 268 nm.

The results indicate that the lyophilisation of the final dialysate yielded 8.5 mg of product as a white powder (yield = 85.1%). HPLC analysis using a mobile phase of acetonitrile and 0.1% trifluoroacetic acid (60:40) at a flow rate of 1 mL/min showed no free AEBSF or other UV light-absorbing contaminants present in the synthesized PG-AEBSF conjugate. Under these HPLC conditions, the free AEBSF was represented by a HPLC peak with a retention time of 3.30 min, while the bound AEBSF in PG-AEBSF was represented by a HPLC peak at 1.70 min (Figure 5). The content of bound AEBSF in PG-AEBSF, estimated by HPLC, was 8.5 % w/w.

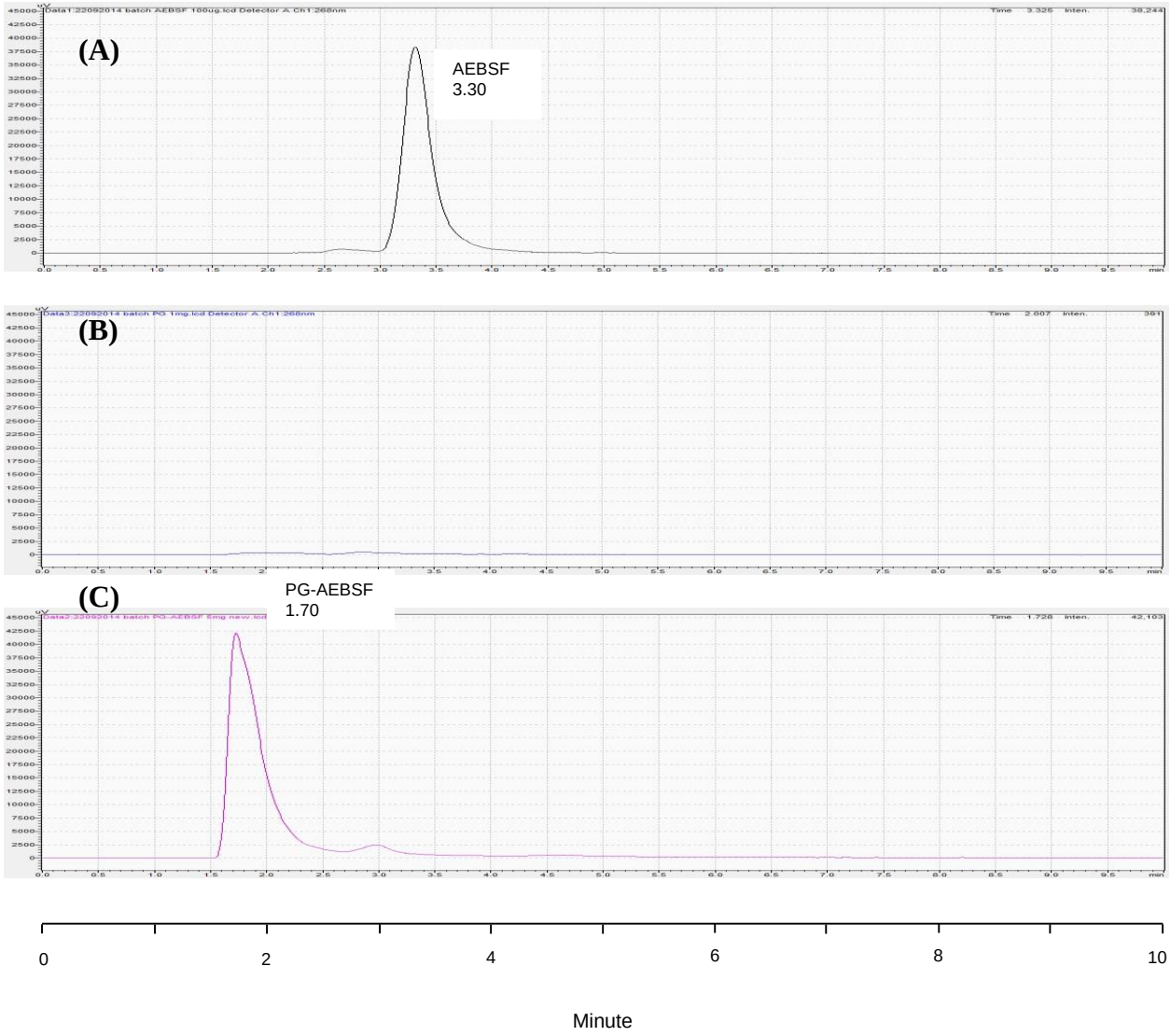

Figure 5 The HPLC chromatograms of (A) 100 µg/mL AEBSF, (B) 1 mg/mL PG, (C) 5 mg/mL PG-AEBSF conjugate.

Abbreviation: HPLC, high performance liquid chromatography; PG, poly-L-glutamic acid sodium salt; AEBSF, 4-(2-aminoethyl)benzenesulfonyl fluoride; PG- AEBSF, poly-L-glutamic acid – 4-(2-aminoethyl)benzenesulfonyl fluoride

^{1}H and ^{13}C NMR analyses were performed on the synthesized PG-AEBSF conjugate, as well as on AEBSF and PG polymer in the proton form, to elucidate the molecular structure of PG- AEBSF and to identify the side group that was involved in the conjugation reaction. The ^{1}H and ^{13}C chemical shifts of the AEBSF and PG (proton form) NMR spectra were assigned to the various proton and carbon atoms. The ^{1}H and ^{13}C chemical shifts of PG-AEBSF NMR spectra were assigned with reference to the assignments for the PG (proton form) and AEBSF (Figure 6).

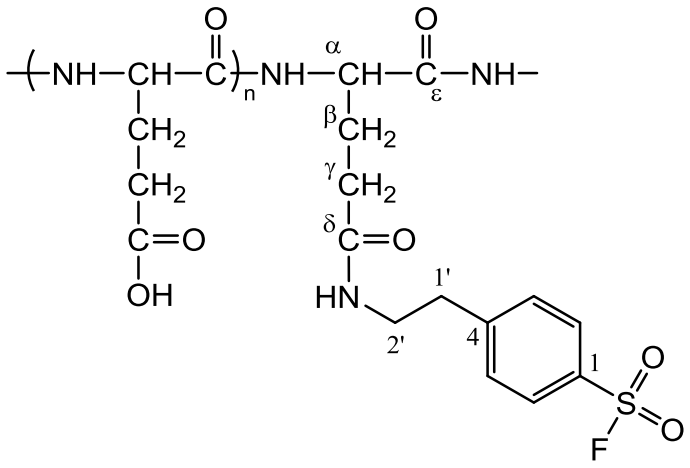

Figure 6 Poly-L-glutamic acid – 4-(2-aminoethyl) benzenesulfonyl fluoride (PG-AEBSF).

^{1}H NMR (D_2O) of 4-(2-aminoethyl)-benzenesulfonyl fluoride (AEBSF), δ (ppm): 8.04 (d, 2H, H–2 and H–6), 7.63 (d, 2H, H–3 and H–5), 3.34 (t, 2H, H–2'), 3.15 (t, 2H, H–1'); ^{13}C NMR (D_2O), δ (ppm): 145.99 (C–4), 130.37 (C–3 and C–5), 130.22 (C–1), 129.01 (C–2 and C–6), 39.85 (C–2'), 32.84 (C–1').

^{1}H NMR (D_2O) of PG-AEBSF, δ (ppm): 8.53 (br s, 1H,PG-NHCO), 7.71 (d, 2H, H–2 and H–6), 7.37 (br s,2H, H–3 and H–5), 4.29 (br s, 1H, H–α), 3.40(br s, 2H, H–2'), 2.79 (br s, 2H, H–1'), 2.25 (m, 2H, H–γ), 2.00 (m, 1H, H–β_a), 1.90 (m, 1H, H–β_b); ^{13}C NMR (D_2O), δ

(ppm): 181.81 (C–δ), 174.10 (C–ε), 143.64 (C–4), 140.99 (C–1), 129.97 (C–3 and C–5), 126.19 (C–2 and C–6), 54.14 (C–α), 41.05 (C–2'), 35.16 (C–1'), 33.93 (C–γ), 28.48 (C–β).

The formation of an amide bond deriving from the conjugation of AEBSF and PG at δ-COOH position was suggested by the evidence from the ^{1}H NMR spectrum. An upfield shift for signal H–1' was observed at 3.15 ppm (AEBSF) to 2.79 ppm (PG-AEBSF). The shielding effect was the result of H–1' experiencing the ring current from the carbonyl moiety of the newly formed amide group.

2.2 Stability of PG-AEBSF and AEBSF in Phosphate-Buffered Saline and Plasma

To study the aqueous stability of AEBSF and PG-AEBSF, 3 mg AEBSF or 4 mg PG-AEBSF was dissolved respectively in 10 mL PBS at pH 7.4 and incubated at 37°C for 120 h. Aliquots (300 µL) were sampled from the respective incubation vials at different time points (0, 0.5, 1, 2, 4, 6, 8, 12, 24, 48, 72, 96 and 120 h). The aliquots were analyzed using reversed phase HPLC as described in the determination of the purity of PG-AEBSF earlier.

To study the plasma stability of AEBSF and PG-AEBSF, similar experiments were repeated by replacing PBS with plasma. Following the sampling, plasma aliquots were mixed with acetonitrile (1:1 v/v) and centrifuged at 14,000 g for 5 min so as to precipitate the plasma proteins.[4] The supernatant was subjected to HPLC analysis.

The protocol for the protein precipitation-HPLC assay for analysis of plasma degradation of AEBSF was validated using six replicates. The limit of quantification (LOQ) of AEBSF in plasma was 0.04 mM. The calibration curve, between 0.04 – 4.00 mM AEBSF, was constructed and its linearity determined. The precision of the concentrations of AEBSF at 0.20, 1.00 and 4.00 mM were between 1.2 and 2.2 RSD, whereas recovery of AEBSF at

the same concentrations was above 90%. The retention times for AEBSF and PG-AEBSF were 3.30 and 1.70 min, respectively.

HPLC analysis showed no significant degradation of PG-AEBSF had occurred in the first 72 h of incubation when incubated in PBS. The release of AEBSF was only observed from 96 h onwards. PG-AEBSF incubated in plasma demonstrated similar release patterns (Figure 7). No other UV-absorbing compound was detected in the incubation mixture. These results suggest that AEBSF is relatively stable and concur with the findings of Xu *et al*.[5] on the stability of AEBSF in aqueous and plasma solution.

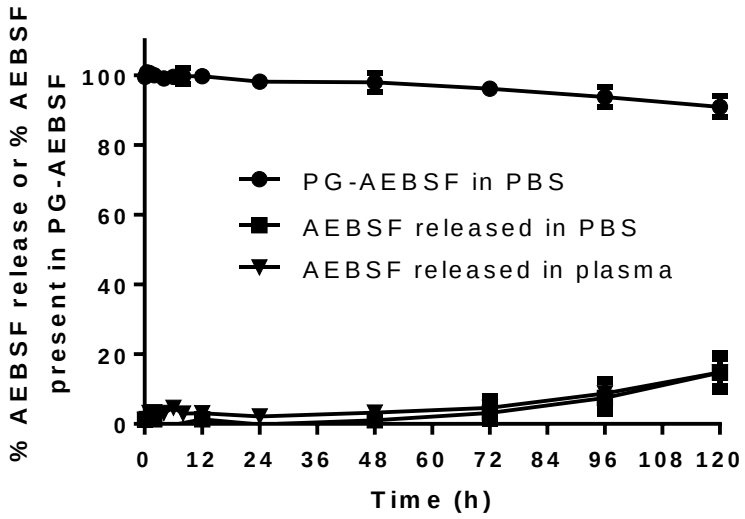

Figure 7 Time dependent release of AEBSF from PG-AEBSF in phosphate buffered saline or plasma at 37°C over a period of 120 h.

Abbreviation: AEBSF, 4-(2-aminoethyl)benzenesulfonyl fluoride; PG- AEBSF, poly-L-glutamic acid – 4-(2-aminoethyl)benzenesulfonyl fluoride

3.0 Characterization of Poly-L-Glutamic Acid – 5-(Aminoacetamido) Fluorescein (PG-AF)

5-(Aminoacetamido)fluorescein (fluoresceinyl glycine amide) (AF) was conjugated to poly-L-glutamic acid (PG)(method as described in main text). The purity and AF content of PG-AF were determined using high performance liquid chromatography (HPLC) as described earlier for PG-AEBSF. The composition of the mobile phase was acetonitrile (ACN) and 0.1% trifluoroacetic acid (TFA) (85:15) with a flow rate of 1 mL/min. The sample volume was 10 μL and monitored using a fluorescence detector (Ex: 445 nm; Em: 530 nm).

The results indicate that the lyophilisation of the final dialysate yielded 8.5 mg of product as a white powder (yield = 82.3%). HPLC analysis showed a small amount of free AF present in the synthesized PG-AF conjugate, and the purity of PG-AF was estimated to be about 92%. Under these HPLC conditions, the free AF was represented by a HPLC peak with a retention time of 4.68 min, while the bound AF in PG-AF was represented by a HPLC peak at 2.70 min (Figure 8). The content of bound AF in PG-AF, estimated by HPLC, was 7.2 % w/w.

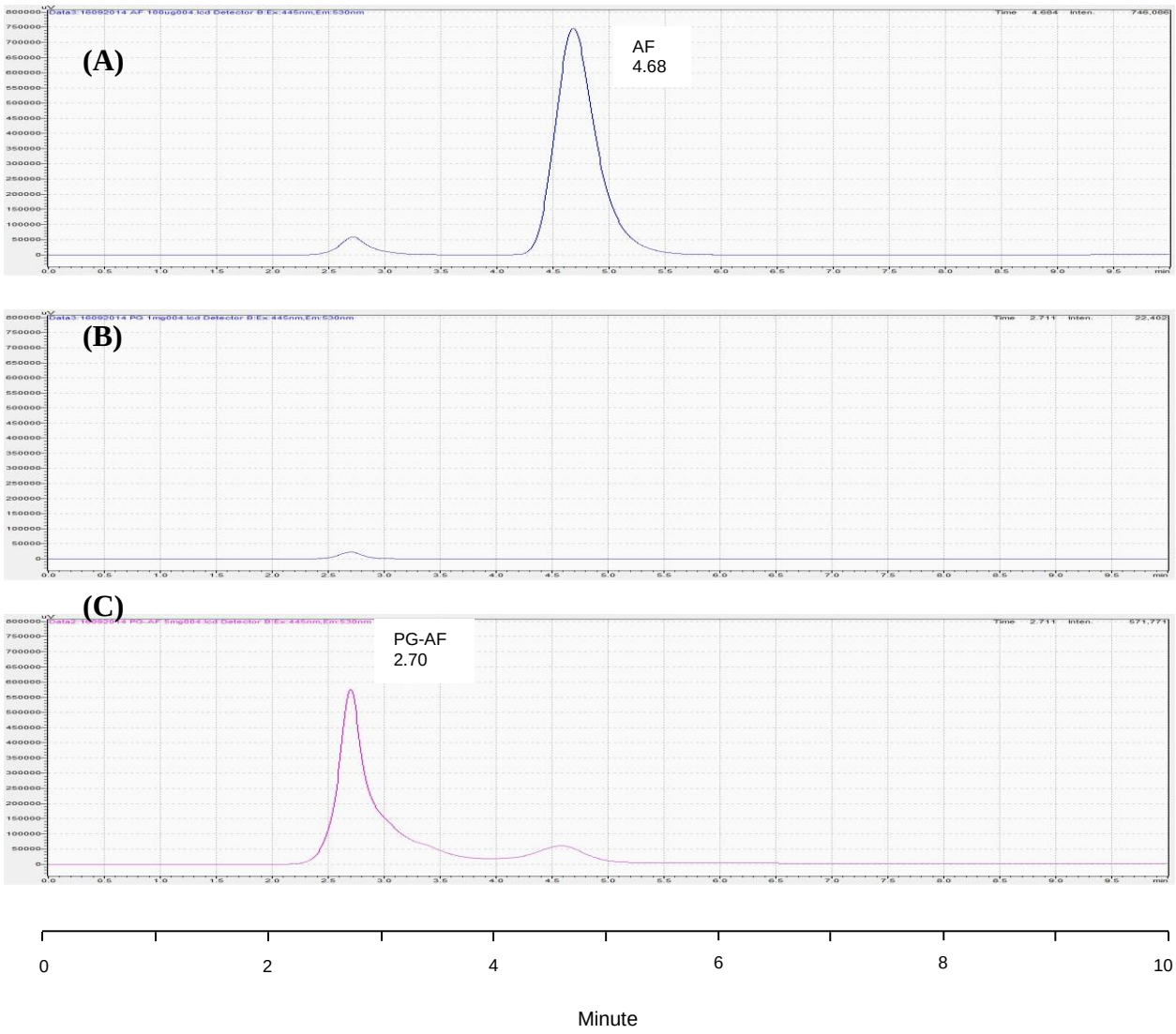

Figure 8 The HPLC chromatograms of (A) 100 µg/mL AF, (B) 1 mg/mL PG, (C) 5 mg/mL PG-AF conjugate.

Abbreviation: HPLC, high performance liquid chromatography; PG, poly-L-glutamic acid sodium salt; AF, 5-(Aminoacetamido)fluorescein; PG- AF, poly-L-glutamic acid 5-(Aminoacetamido)fluorescein

^{1}H and ^{13}C NMR analyses were performed on the synthesized PG-AF, as well as on the AF and PG polymer in the proton form, to elucidate the molecular structure of PG- AF and to identify the side group that was involved in the conjugation reaction. The ^{1}H and ^{13}C chemical shifts of the AF and PG (proton form) NMR spectra were assigned to the various proton and carbon atoms. The ^{1}H and ^{13}C chemical shifts of PG-AF NMR spectra were assigned with reference to the assignments for the PG (proton form) and AF (Figure 9).

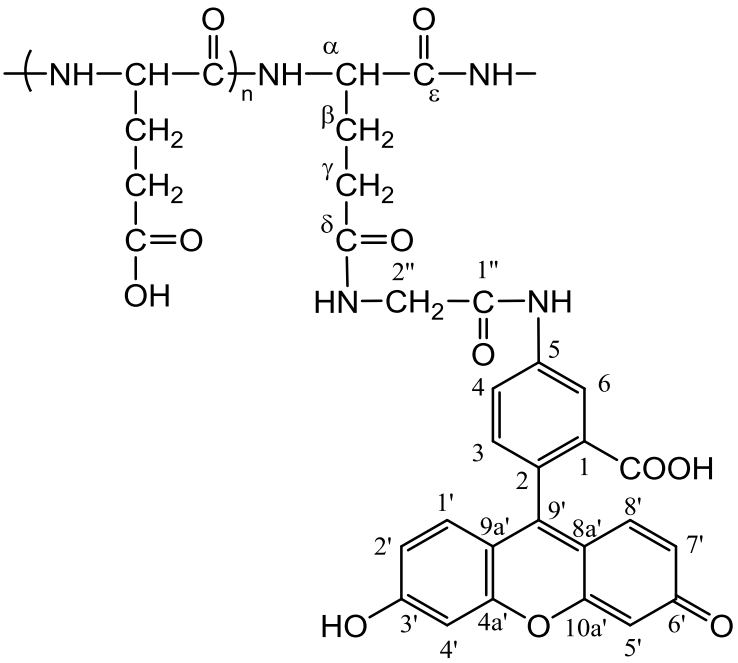

Figure 9 Poly-L-glutamic acid-5-(aminoactamido) fluorescein (PG-AF).

^{1}H NMR (*d*-DMSO) of 5-(aminoacetamido)fluorescein (AF), δ (ppm): 8.35 (d, 1H, H–6), 7.86 (dd, 1H, H–4), 7.18 (d, 1H, H–3), 6.65 (d, 2H, H–4’ and H–5’), 6.58 (d, 2H, H–1’ and H–8’), 6.53 (dd, 2H, H–2’ and H–7’), 3.36 (s, 2H, H–2”) ;^{13}C NMR (*d*-DMSO), δ (ppm): 172.63 (C–1”), 168.87 (COOH), 160.08 (C–3’), 152.21 (C–4a’ and C–10a’), 146.37 (C–5), 140.51 (C–2), 129.26 (C–1’ and C–8’), 127.53 (C–1), 126.40 (C–4), 124.75 (C–3), 113.94 (C–6), 113.02 (C–2’ and C–7’), 109.96 (C–8a’ and C–9a’), 102.40 (C–4’ and C–5’), 45.46 (C–2”) .

^{1}H NMR (*d*-DMSO + D_2O) of PG-AF, δ (ppm): 7.65 (1H, d), 6.36 (d, 1H), 5.82 (dd, 1H), 3.51 (br s, 1H, H–α), 2.91 (s, 2H), 1.47 (m, 2H, H–γ), 1.27 (m, 1H, H–β_a), 1.14 (m, 1H, H–β_b);^{13}C NMR (*d*-DMSO + D_2O), δ (ppm): 190.69, 185.42 (C–δ), 178.13 (C–ε), 170.30, 164.69, 163.08, 143.30, 136.07, 134.86, 126.83, 107.76, 71.21, 58.42 (C–α), 38.23 (C–γ), 32.61 (C–β) .

Although the NMR signals of PG-AF were not sufficiently well resolved, the presence of NMR signals from both PGH and AF in PG-AF clearly suggested AF was conjugated to PGH. This was supported by the HPLC chromatograms (Figure 8), which indicated that the retention time of PG-AF was at 2.70.

3.2. Stability of PG-AF and AF in Phosphate-Buffered Saline and Plasma

Similarly, aqueous stability of AF and PG-AF in both phosphate-buffered saline and plasma was determined using the methods described above.

The limit of quantification of AF in plasma was 0.025 mM. The calibration curve, between 0.025 – 2.50 mM AF, was constructed and its linearity determined. The precision of AF concentrations at 0.10, 1.00 and 2.50 mM were between 1.5 and 2.5 RSD, while AF recovery at the same concentrations was above 90%. The retention times for AF and PG-AF were 4.68 and 2.70 min, respectively. The stability of PG-AF in plasma appeared to be similar to PG-AEBSF, up to the 48 h time point (Figure 10).

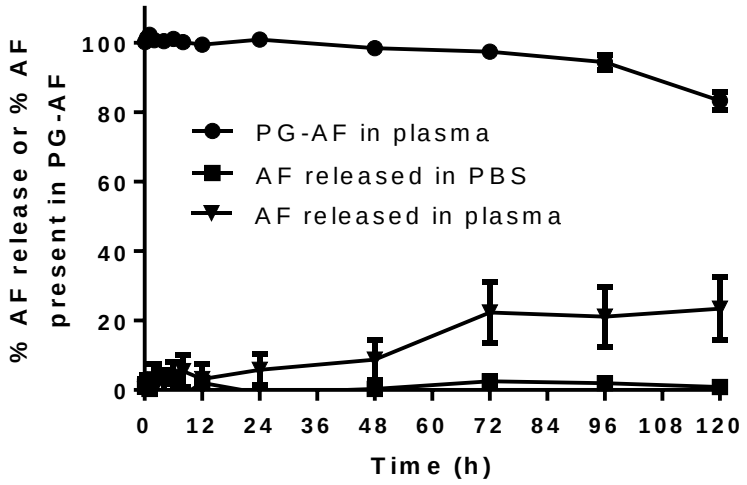

Figure 10 Time dependent release of AF from PG-AF in phosphate buffered saline or plasma at 37°C over a period of 120 h.

Abbreviation: AF, 5-(Aminoacetamido)fluorescein; PG- AF, poly-L-glutamic acid 5-(Aminoacetamido)fluorescein

4.0 Determination of Oxidative Stress Levels and Kidney-Body Weight Ratio Changes in Normal and Diabetic Rats

Prior to the biodistribution study of PG-[^{3}H]dCyd, renal cellular changes were assessed based on the kidney-body weight ratio 2 weeks after diabetes induction [6]. Rats (n=6) were weighed and then sacrificed using an overdose of anesthetic (i.p. injection of 100 mg/kg sodium pentobarbital) and kidneys removed. The kidney-body weight ratio was calculated according to the formula:

$$\frac{\text{Kidney weight}}{\text{Body weight}} \quad \text{X } 100\ \%$$

Renal oxidative stress levels in diabetic rats were determined via the Ferric Reducing Ability of Plasma (FRAP) assay.[7] Briefly, kidney samples were homogenized in ice cold saline (1:10 w/v) and centrifuged at 2000 x g for 10 minutes at 4°C. Twenty microliters of supernatant were added to 20 µL of distilled water and 250 µL of freshly prepared FRAP working reagent. The solution was then incubated at 37°C for 4 minutes. The mixtures were subjected to spectrophotometric analysis (λ = 593 nm) using varying concentrations of Fe^{3+} (100 to 1000 mM) solutions as standards and an acetate buffer as blank. The FRAP value was calculated using the following formula and expressed in mM Fe^{2+}:

FRAP value (mM Fe^{2+}) = (absorbance for sample or standard – absorbance for sample blank)/0.001, where 0.001 is the constant derived from the standard curve. Diabetic rats (n = 5) were compared to normal rats (n = 5) kept under similar conditions.

The renal oxidative stress levels and kidney-body weight ratio of the diabetic rats were increased by 40% and 100%, respectively, when compared to normal rats (Student's t-test, both $p < 0.01$, Figure 11 and 12). These results coincide with previous findings on the

development of oxidative stress[8, 9] and increase in kidney mass due to renal cellular changes, such as proximal tubule degradation and fibrosis,[6] in diabetes. Therefore, the data support the use of this diabetic rat model to assess PG biodistribution and renal targeting.

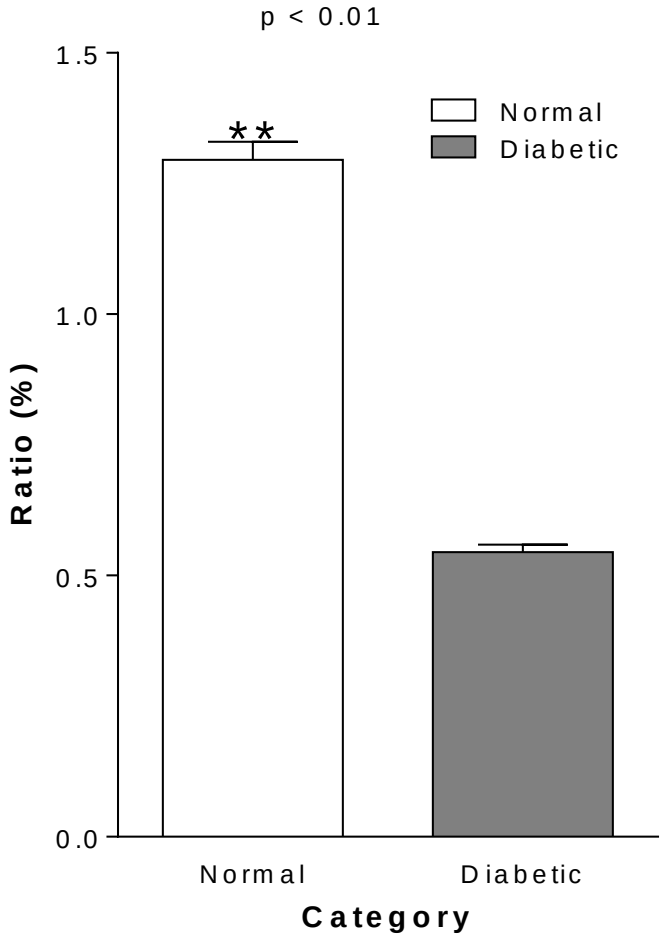

Figure 11 The kidney-body weight ratio of the diabetic rats was increased by 100%, when compared to that of the normal rats. Results are shown as the mean ± SEM (n = 5). ** P < 0.01 when compared with the control, Student's t-test.

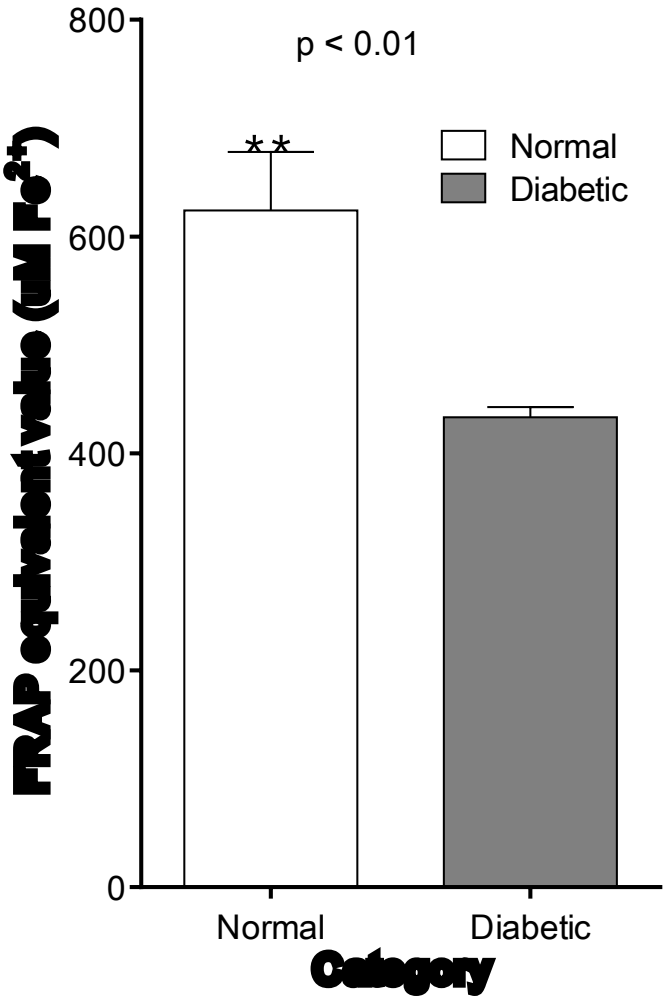

Figure 12 The renal oxidative stress levels of the diabetic rats were increased by 40% when compared to that of the normal rats. The results are shown as the mean ± SEM (n = 5). ** P < 0.01 when compared with the control, Student's t-test.

References

1. Kiew LV, Cheong SK, Sidik K, Chung LY. Improved plasma stability and sustained release profile of gemcitabine via polypeptide conjugation. Int J Pharm 2010 May 31;391(1-2):212-20.
2. Kiew LV, Cheong SK, Ramli E, Sidik K, Lim TM, Chung LY. Efficacy of a Poly-L-Glutamic Acid-Gemcitabine Conjugate in Tumor-Bearing Mice. Drug Development Research 2012;73(3):120-29.
3. Pelet JM, Putnam D. An In-Depth Analysis of Polymer-Analogous Conjugation using DMTMM. Bioconjugate Chemistry 2011 2011/03/16;22(3):329-37.
4. Haas R, Rosenberry TL. Protein Denaturation by Addition and Removal of Acetonitrile: Application to Tryptic Digestion of Acetylcholinesterase. Analytical Biochemistry 1995;224(1):425-27.
5. Xu Q, Zhang Y, Trissel LA. Physical and chemical stability of gemcitabine hydrochloride solutions. J Am Pharm Assoc (Wash) 1999 Jul-Aug;39(4):509-13.
6. Liu S, Barac-Nieto M. Renal protein degradation in streptozotocin diabetic mice. Diabetes research and clinical practice 1997 Jan;34(3):143-8.
7. Benzie IFF, Strain JJ. The Ferric Reducing Ability of Plasma (FRAP) as a Measure of "Antioxidant Power": The FRAP Assay. Analytical Biochemistry 1996;239(1):70-76.
8. Greene DA, Stevens MJ, Obrosova I, Feldman EL. Glucose-induced oxidative stress and programmed cell death in diabetic neuropathy. European journal of pharmacology 1999 Jun 30;375(1-3):217-23.
9. Vasavada N, Agarwal R. Role of oxidative stress in diabetic nephropathy. Advances in chronic kidney disease 2005;12(2):146-54.